Early glaucoma screening Decision Tree using in-depth clinical analysis of the optic nerve head

Rostom Kachouri, Mohamed Akil, Amed Mvoulana

Early glaucoma screening Decision Tree using in-depth clinical analysis of the optic nerve head

Rostom Kachouri
Gaspard Monge Computer Science Laboratory, ESIEE-Paris, Gustave Eiffel University, France
rostom.kachouri@esiee.fr

Mohamed Akil
Gaspard Monge Computer Science Laboratory, ESIEE-Paris, Gustave Eiffel University, France
mohamed.akil@esiee.fr

Amed Mvoulana
Gaspard Monge Computer Science Laboratory, ESIEE-Paris, Gustave Eiffel University, France
amed.mvoulana@esiee.fr

***Abstract*—: To assess the performance of an end-to-end computer vision algorithm for the early screening and diagnosis of glaucoma from fundus photographs. Development and evaluation of a computer vision approach for the extraction of physiologic measurements from the optic nerve head (ONH) and the detection of glaucoma. 101 fundus photographs were included for the development and validation of the screening algorithm. We automatically detect and extract the ONH within the retina, and compute two methods for segmenting of the optic cup (OC) and the optic disc (OD). Referable ophthalmic features including the cup-to-disc ratio (CDR), the Inferior- Superior-Nasal-Temporal (ISNT) rule and the neuroretinal rim (NRR) area are exploited, to quantify the structural changes within the ONH. Then, we elaborate a clinical protocol to provide trustworthy, easily interpretable glaucoma screening process, and indications about the stages of disease spreading.**

Proposed approach allows to accurately estimate the clinical measurements with 0.11 ± 0.08 to 0.15 ± 0.12 mean-std error rates on CDRs, ISNT sectors and NRR area. Also, outstanding glaucoma screening performance was achieved with 93.07% (95% confidence interval (CI), 86.24% to 97.17%) accuracy, 98.57% (95% CI, 92.30% to 99.96%) sensitivity and 80.65% (95% CI, 62.53% to 92.55%) specificity rates, competing with the state-of-the-art. We formulated a clinical protocol aiming at evaluating the structural changes occurring within the ONH, for assessing the different spreading stages of the neuropathy. Excellent performance has been obtained on glaucoma screening process, allowing to integrate such algorithm into computer-aided diagnosis systems and support ophthalmologists.

Keywords— Glaucoma screening, Computer-aided diagnosis (CAD), Retinal fundus images, Optic nerve head (ONH), optic cup (OC), optic disc (OD), cup-to-disc ratio (CDR), Inferior-Superior-Nasal-Temporal (ISNT) rule, Neuroretinal Rim (NRR) area.

I. INTRODUCTION

Glaucoma is one of the most prevalent ocular diseases worldwide, and the second leading cause of blindness in the Globe [1]. The development of the disease is highlighted by inflicting progressive loss of visual field, leading to blindness in critical circumstances [2] (see Figure 1).

(a) Healthy (b) Early (c) Moderate (d) Advanced

Fig. 1. Differences between healthy (a) and glaucomatous (early (b), moderate (c) and advanced (d)) vision: glaucoma induces a gradual narrowing of the field of view, until complete blindness for critical incurred cases.

Because of the asymptomatic traits of the disease at earlier stage, patients are often unaware of suffering from glaucoma until the pathology reaches advanced stage, undergoing with dramatical and irreversible visual disturbance. Hence, early screening and diagnosis of glaucoma is the key to curb glaucoma development and prevent from the induced irreversible ocular disorders, and then provide in-time treatment, dedicated clinical care and follow-up allowing to sustainably maintain visual functions.

Glaucoma is generally diagnosed with a bunch of clinical tests conducted by the ophthalmologist, including: visual field control (i.e. perimetry), IOP measurement (operated with a tonometer, and aims at detecting an unusual increased pressure within the eye, possibly related to glaucoma) and retinal examination. However, visual field assessment is not an adequate control for early screening and diagnosis of glaucoma, since clinical disturbances occur at advanced and irremediable stages. Otherwise, increased IOP is neither a necessary nor sufficient criterion for assessing the presence of the disease, since glaucoma could manifest itself without an increased pressure [3].

Retinal examination consists in assessing the optic nerve head (ONH) and its surroundings, and detecting eventual lesions and defects related to the neuropathy [4]. Indeed, fundus photography has longer been, and remains the main used imaging tool for assessing the retina. It consists in a 2D-acquisition of retinal surface, highlighting the different parts of the retina such as the ONH, the macula and the retinal vasculature. Fundus photography then allows to inspect ONH (bright circular area on the surface of the retina) topography, by extracting quantitative measurements related to optic cup (OC) and optic disc (OD) structures for glaucoma assessment (see Figure 2, (b)). Evaluation of the retina has been recognized by prominent studies in ophthalmology as a more reliable way for screening the presence of glaucoma at its earlier stage. Automated early screening and diagnosis of glaucoma from retinal fundus images involves the computation of measures and shape features, for evaluating the structural changes within and around the ONH in a longitudinal manner [5].

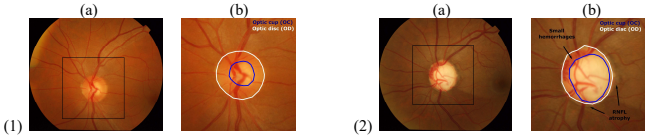

Fig. 2. Example of healthy (1) and glaucomatous (2) retinal images: (a) Retinal image with framed ONH region, (b) ONH sub-image. In (1) regular OC size inside the OD, no RNFL loss and hemorrhages are apparent. In (2), there is a prominent cupping inside the OD, localized RNFL loss around the ONH, tiny and localized hemorrhages inside the NRR.

In this work, our main contributions are to lead an in-depth clinical analysis of glaucoma, through the ONH structural changes caused by the rise, the evolution and the spreading of the neuropathy; to establish comprehensive relationships between the development of glaucoma and well-known referable ophthalmic measurements related to the presence of the disease. Developed solutions give arise to intelligent, accurate and interpretable diagnosis-help systems, offering ophthalmologists, optometrists, and trained medical professionals guidance on the pathway to screening glaucoma, and widespreading eye health services through useful mass screening programs.

The remainder of this paper is organized as follows. Section II reviews the current work conducted by state-of- the-art methods for the screening of glaucoma, using the well-known and reliable clinical measurements. Based on this thorough investigation of the literature, Section III gives a prior in-depth clinical analysis of glaucoma and the correlated morphological alterations of the ONH, and introduces the path forward identifying glaucomatous patterns with the ONH measurements. Thereupon, proposed methods are described in section IV. Overall contributions and reached results are discussed in section V. Finally, conclusions are addressed in section VI.

II. Related works

In the field of biomedical engineering, fully-automated screening and diagnosis of glaucoma from retinal fundus involves the computation of clinical measurements, to quantify the alteration of ONH topography and the structural changes induced by the neuropathy along its different stages. Among several attributes formulated in the state-of-the-art, the cup-to-disc ratio (CDR), the inferior-superior-temporal-nasal (ISNT) rule and the NRR area have been widely exploited for the diagnosis of the pathology, and validated by specialists as relevant indicators to analyse the structural changes of the ONH, then assess the presence of glaucoma disorder. From a clinical point of view, these attributes and measures allow to early detect the presence of the disease, monitor its progression over time, and then deliver an effective treatment to blunt its spread and avoid visual loss. These measures allow to undertake in-depth examination of the ONH, and are easily interpretable by the specialist to deliver a diagnosis of the presence of the pathology. To compute these measurements from retinal fundus images, a joint OC-OD segmentation is required. Hence, precise calculation of the intended features for glaucoma screening directly depends on an accurate segmentation of both OC and OD regions. In this context, many methods have been introduced in the literature, performing joint OC-OD segmentation for further glaucoma assessment with the exposed referable measurements. A summary of the state-of-the-art is outlined in Table I.

In this work, we answer the lacks of existing methods, as these clinical measurements are not systematically provided or not combined to automatically deduce the most adequate association for a better diagnosis. Hence, this work aims at delivering a thorough analysis of structural-to-functional damages caused by glaucoma, by studying the induced structural changes of the ONH and their link with well-known clinical measurements. In this direction, we give an in-detailed explanation of retinal structure and how the glaucomatous neuropathy impacts the topography of the ONH along its progression, and their relationship with referable ophthalmic features. After a thorough explanation on how to extract such measurements from a geometrical and image processing aspect, we provide reliable measurement of the clinical features, and establish a clinical protocol towards glaucoma assessment.

III. In-depth clinical analysis of glaucoma

Glaucomatous neuropathy manifests itself within the retinal layer, across optic nerve head (ONH) zone. Its progressive development leads to a gradual alteration of the visual field. These visual disturbances have been shown to be intrinsically correlated with the structural alterations of the ONH, responsible for transmitting the received light information to the brain. The ONH is made up of the convergence of the optical fibers, and comprises the OC, appearing as a whitish central depression, surrounded by the OD appearing as a circular peripheral area. The NRR emerges itself outside the OC, inside the disc. The basic structural changes occurring within the ONH mainly consist in a gradual growing of the OC area inside the OD area, also called cupping, inducing an antagonist thinning of the NRR. The gradual widening of the cupping is also featured by a specific growth of the OC across its longitudinal and transversal directions. Evaluation of these structural changes through clinical measurements of the ONH components allows to early feature the glaucomatous patterns.

TABLE I. Summary of the state-of-the-art methods for glaucoma screening from retinal images: authors, clinical measurements, advantages and limitations.

Authors	Clinical measurements	Advantages	Limitations
Nayak et [6] al.	Diameter-based CDR, ISNT rule	The use of different measurements to feature to assess the presence of the disease	The use of a neural network classifier, decreasing the ability in interpreting the diagnosis
Cheng et [7] al.	Diameter-based CDR	Accurate segmentation of the OC and the OD through a supervised classification method	The use of a single feature for glaucoma screening, with a fixed threshold value
Das et al. [8]	Diameter-based CDR, ISNT rule	The use of different measurements to assess the presence of the disease	A few explanations on how to combine the features for glaucoma screening, no indications about the spreading stage of glaucoma
Diaz-Pinto al.Et [9]	Area-based and diameter- based CDR, ISNT rule	Accurate segmentation phase through a color space comparative study, the use of three clinical features for glaucoma assessment	A few explanations on how to combine the features for glaucoma screening, no indications about the spreading stage of glaucoma
Mvoulana al.Et [10]	Area-based CDR	Accurate segmentation of the OC and the OD with a non-supervised method, accurate glaucoma screening process	The use of a single feature for glaucoma screening, with a fixed threshold value
Kumar et [11]al.	Rim-to-disc ratio (RDR)	The use of a brand-new NRR-derivated feature, indications about disease severity with DDLS indicator	The use of a single feature for glaucoma screening, a few explanations about the clinical aspect of glaucoma

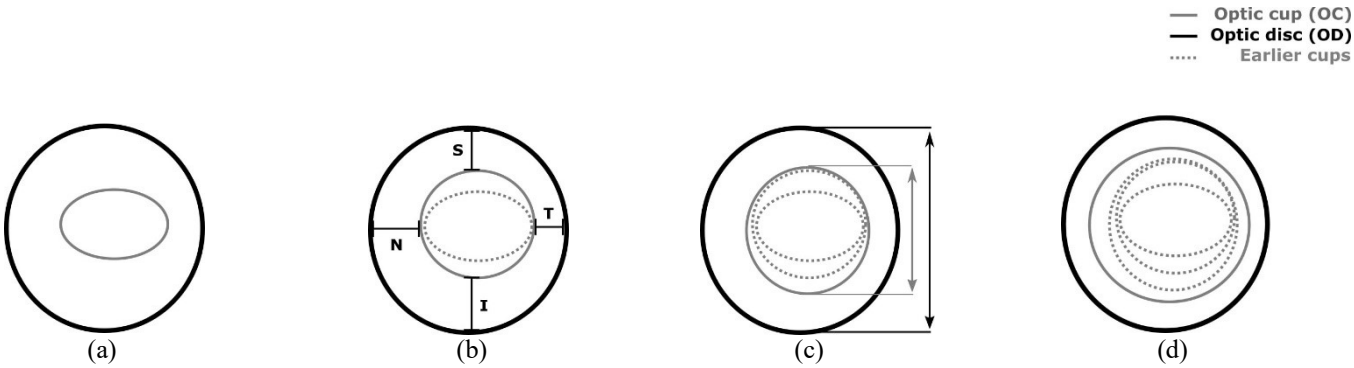

Fig. 3. Evolution of glaucoma during time, in concordance with the structural changes occurring within the ONH along the different stages of the disease: (a) healthy patient, (b) glaucoma at its earlier stage, (c) glaucoma at its moderate stage, (d) glaucoma at its advanced stage. Clinical measurements (area-based CDR, diameter-based CDR, ISNT rule, NRR area) allow to discriminate the different stages of development of the disease. Optic cup (OC) appearing on dashed line refers to the previous stages.

In the presence of a healthy case (see Figure 3, (a)), OC size inside the OD does not exceed a certain proportion of the disc, fewer than half the OD area [48]. Also, in most cases, OD has an oval shape along the vertical axis, while the OC tends to be oval along the horizontal axis. The NRR follows a precise configuration: the rim is thicker along the inferior sector (6 o'clock), then along the superior sector (12 o'clock), followed by the nasal (9 o'clock) and temporal sectors (3 o'clock). In normal controls, NRR show off an area higher than half the OD area.

In the presence of a pathological case, morphological evolution of ONH structures is observed, and several configurations are upset. The major sign to detect the disease is the progressive widening of the OC within the OD, until the usual cup proportions from a healthy patient are exceeded (see Figure 3 (b), (c) and (d)). The appearance or accentuation over time of this sign induces a progression of the neuropathy, and excessive preponderance of the OC within the disc allows to discriminate the pathological cases (see Figure 3 (d)). Also, the enlargement of cup area is generally faster along the vertical axis than along the horizontal axis, inducing a vertical elongation of the cup area (see Figure 3 (c)). Measuring and monitoring this elongation over time allows a more accurate tracking of patients with glaucoma at moderate-to-advanced stage of structural changes. At advanced stages of the disease, the cup tends to grow uniformly in both directions, and the surface criterion helps reaching better recognition of glaucomatous cases. Finally, a disruption of the configuration of rim thickness is also observed in certain pathological cases: it becomes abnormally thinner in the lower and upper sections (see Figure 3 (b)). The upheaval of this rule allows the detection of the few earliest cases of the pathology.

Figure 4 illustrates the different extracted measures, allowing to evaluate the structural changes of the ONH and determine whether a subject is potentially suffering from glaucoma with the formulated criteria.

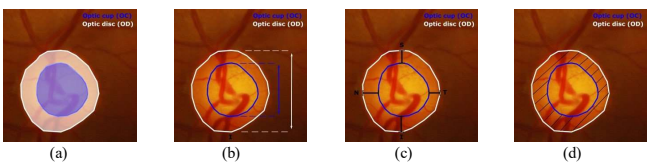

Fig. 4. Extracted features for the clinical evaluation of the ONH: (a) OC and OD areas for area-based CDR, (b) OC and OD vertical diameters for diameter-based CDR, (c) ISNT sectors for ISNT rule, (d) NRR area.

Area-based CDR corresponds to the ratio of the area of the OC and the area of the OD (see Figure 4, (a)). Diameter- based CDR, on his side, corresponds to the ratio of the vertical diameter of the OC and the vertical diameter of the OD (see Figure 4, (b)). Both quantify the amount of cupping within the ONH, and the preponderance of the OC inside the OD, respectively in a 1-D and a 2-D manner with longitudinal and surface study.

In either case, such measures allow distinguishing healthy subjects (with lower CDR value) from subjects suffering from moderate-to-advanced glaucoma (with greater CDR value), as well as monitoring the progression of the disease [7, 12]. On the one hand, area-based CDR aCDR is measured by computing the ratio between the area AOC of the OC region, and the area AOD of the OD:

$$aCDR = \frac{A_{OC}}{A_{OD}} \tag{1}$$

In biomedical engineering and image processing, the area of both regions is expressed as the number of pixels belonging to each zone. The ratio then allows to obtain a normalized factor, further exploited to detect glaucomatous discs. On the other hand, diameter-based CDR vCDR is defined as the ratio of the vertical diameter DOC of the OC and the vertical diameter DOD of the OD:

$$vCDR = \frac{D_{OC}}{D_{OD}} \tag{2}$$

The ISNT sectors for ISNT rule refer to the inferior IS, superior SS, nasal NS and temporal TS sectors. Each sector represents the distance between the borders of the OC and the OD, according to the four quadrant directions (see Figure 4, (c)). In our study, the sectors are measured as the distance between the edges of each bounding box around the OC and OD areas, along the four directions. As for calculating the area-based and diameter-based CDR, each distance is expressed then compared in pixels. With healthy subjects, the rule is obeyed as the sectors are greater inferiorly, then superiorly, then nasally, and temporally [13]. With suspicious subjects, the rule tends not to be obeyed. The ISNT rule can be modelized as:

$$ISNT = \begin{cases} obeyed, & I_S > S_S > N_S > T_S \\ not\ obeyed, & otherwise \end{cases} \tag{3}$$

However, prior knowledge about nasal and temporal sectors, depending on the captured eye (right or left), is most of the time a missing information from the processed retinal

images. Thus, in concordance with relevant studies exploiting the ISNT rule for glaucoma screening, an adaptation of the rule is operated by considering two sub-rules ISN and IST [14]. ISNT criterion is then defined as:

$$ISNT = ISN \cap IST = \begin{cases} obeyed, & I_s > S_S > N_S \quad and \quad I_s > S_S > T_S \\ not\ obeyed, & otherwise \end{cases} \quad (4)$$

Finally, the NRR area refers to the area of the rim included in the OD zone, outside the OC (see Figure 4, (d)). NRR area NRRa is then defined as:

$$NRRa = A_{OD} - A_{OC} \quad (5)$$

where AOD and AOC denotes the respective area of the OD and the OC, expressed as the number of pixels belonging to each region.

Consequently, we firstly propose in this paper a brand-new approach for the clinical evaluation of the ONH from retinal fundus images. Here, we leverage the challenge of segmenting the OC and OD regions in a precise manner, for further assessment of the ONH through ophthalmic measurements. In this way, we formulate two segmentation pipelines, and carefully analyse their impact and reliability on the estimation of the clinical features, but also alongside glaucoma screening route. We secondly employ these clinical measurements to propose accurate early screening and diagnosis of glaucoma, combining them to consider all the morphological alterations of the ONH when glaucoma spreads. Provided clinical strategy allows final glaucoma assessment of the glaucomatous neuropathy, and gives crucial indications to the specialist about the prevailing stage of the disease.

IV. Proposed Methods for the Clinical Evaluation of the Optic Nerve Head

The clinical evaluation of the ONH from retinal fundus images implies the segmentation of the OC and OD regions. The intended segmentation process has a critical importance for quantitatively evaluate the structural changes of the ONH with the clinical measurements, for the assessment of glaucoma. Hence, automated evaluation of the ONH from retinal images involves the subsequent stages: prior detection and extraction of the ONH, joint OC-OD segmentation and extraction of clinical features. The flowchart of the overall proposed method for glaucoma screening from retinal fundus images is illustrated in Figure 6.

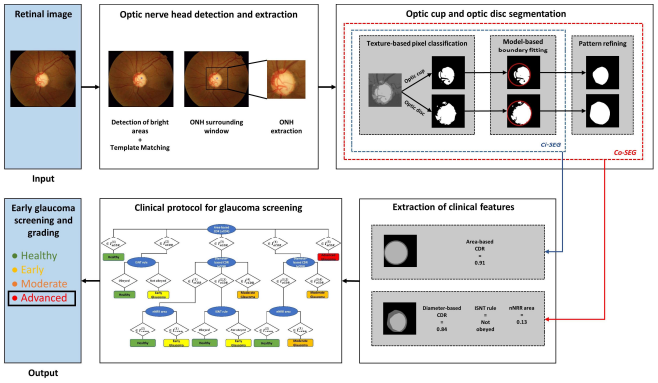

Fig. 5. Flowchart of the proposed method for glaucoma screening and diagnosis: optic nerve head (ONH) detection and extraction, optic cup (OC) and optic disc (OD) segmentation, extraction of clinical features and clinical protocol for glaucoma screening. In this example, the proposed clinical protocol allows a reliable assessment of an advanced glaucoma.

A. Prelude: Benchmark datasets

Publicly-available DRISHTI-GS1 dataset [15] has been used as a standard retinal image dataset for the evaluation of our proposed methods, on the pathway to clinical evaluation of the ONH for glaucoma screening. The dataset consists of 101 retinal color images from a cohort of 101 patients. The retinal images were collected at Aravind Eye Hospital, Madurai, India, with full consent of residents. On the one side, glaucomatous subjects were selected by clinical investigators, based on structural-to-functional clinical findings. On the other side, patients not found to be glaucomatous along refraction test and retinal examination were assigned to the healthy class. Overall selected patients were between 40-80 years with equally-distributed gender. The images were captured with dilated eye, 30-degree field-of-view (FOV), ONH centered, each image made up of a high 2896 × 1944 resolution.

For each retinal image, ground-truth collection has been operated by four well-experienced and trained ophthalmologists, providing OC and OD segmentation and glaucoma assessment. First, the manual marking of each OC and OD boundaries was computed by the four ophthalmologists, with a dedicated and well-designed computer-aided tool.

B. Optic nerve head detection and extraction

Detecting and extracting the ONH from retinal fundus images plays a substantial role towards identifying ocular disorders, such as diabetic retinopathy or glaucoma. However, locating the ONH in a precise manner within the retina is challenging due to various constraints: individual differences, uneven illumination, or variation in ONH appearance and shape [16]. In particular, ONH localization may be complex in the presence of bright lesions on the retinal layer, caused by pathological conditions.

To answer the drawbacks of these respective methods, our ongoing work for ONH detection is based on our previous contributions [10]. First, the detection of the bright regions allows to localize the center of each bright area appearing in retinal layer, including the ONH and eventual bright lesions caused by specific pathological conditions. In this direction, image processing techniques including histogram equalization, thresholding and distance transform are successively applied to the retinal image, leading to the detection of the brightness peaks. Then, from the center of each detected area, template matching is operated to find the actual position of the ONH among the detected centers. Predicted ONH position then corresponds to the area reaching the maximum likelihood with the template, among all detected bright points within the retina. The global approach finally allows to robustly detect the nerve head, even in the eventual presence of lesions. From the detected location, the sub-window is extracted, thereafter leading to ONH examination for glaucoma screening.

C. Optic cup and optic disc segmentation

Segmenting the OC and the OD is a key stage when conducting the evaluation of glaucoma, for assessing the structural changes occurring within the ONH related to the visual disturbances caused by the neuropathy. However, leading joint OC-OD segmentation process is challenging, due to several constraints this medical context brings on:

structures with not well-defined boundaries, individual differences, variations in image acquisition, etc. To carry out this task, we introduce two efficient methods for segmenting the cup and the disc. Starting from the extracted ONH sub-image, the segmentation approach consists of the three following steps: texture- based pixel classification, model-based prior boundary fitting and convex hull transform.

In this segmentation context, the K-means clustering algorithm is employed using an intensity-based nearness criterion. Thus, this approach allocates each area of the retinal sub-image among K clusters following its gray-level. Since the main retinal components are the OC, the OD, the background and the blood vessels, a fixed value K = 4 is selected. Appliance of the K-means clustering algorithm then gathers all pixels belonging to the same retinal structures. Then, since the OC and the OD are the retinal structures with the greatest gray-level in the ONH sub-image, they are both associated to the two cluster centers with the two greatest gray-level values. Thus, the cluster with the greatest intensity corresponds to the OC, when the second greatest intensity corresponds to the NRR (OD without the cup). The gathering of each region finally forms the OD. To remedy the non well-defined boundaries of OC and OD, we compute a circle-based fitting of the regions since the regions are known for their circular feature, and then finding circular shapes in the image. Finally, from the computed circle fitting, only the white pixels inside the detected circle are considered as part of the segmented OC and OD areas. To smooth final segmentation, we operate a well-known image processing technique, called convex hull transform, which consists in computing the convex hull of all white pixels inside the circle.

Hence, the first segmentation method derives from the detected circular regions after a Model-based boundary fitting, where a circularity-based segmentation (Ci-SEG) approach is employed [10]. Thereupon, the second segmentation method derives from the detected convex regions after a Pattern refining, where a convexity-based segmentation (Co-SEG) approach is employed. The basic idea behind proposing two parallel pipelines is to enhance our ability to extract the clinical measurements, for ensuring glaucoma screening process.

D. Clinical protocol for glaucoma screening

After OC and OD segmentation, clinical features are extracted for further detection of the subjects suffering from glaucoma. The aim is to establish a clinical protocol, bringing together the extracted clinical features as a specialist would carry out its examination of the ONH, to assess the structural changes linked to the presence of glaucoma. To do so, we first analyze the ability of these attributes to discriminate healthy patients from patients suffering from glaucoma, through their sensitivity and specificity in screening pathological subjects. This study is conducted with both Ci-SEG and Co-SEG segmentation approaches, to enhance our ability to extract the intended features and improve the capacity of each feature to detect the disease with the most adapted segmentation approach. Given their relationship with glaucoma progression, and their intrinsic capacity in discriminating such glaucomatous patterns, we articulate a clinical arborescence, describing the clinical pathway on disease screening. Hence, the arborescence finally contributes to reliable assessment of glaucoma, exploiting the clinical features and combining them in a hierarchical manner to screen the disease and give indications about the different stages of disease spreading (early, moderate, advanced).

V. DISCUSSION AND OBTAINED RESULTS

Given our thorough study, the proposed clinical protocol for glaucoma screening is a hierarchical arborescence (Decision Tree). Since the area-based CDR is the most relevant feature to discriminate the presence of glaucoma, it appears on top of the arborescence and is the first feature to explore when evaluating the ONH morphological evolution. Given the value obtained on area-based CDR across different intervals of values to study. Reached values on area-based CDR are divided into 5 intervals of study $I^{(i)}_{aCDR}$, corresponding to the different phases of disease development according to the International Classification of Diseases (ICD) [17]:

$$I^{(1)}_{aCDR} = [0; 0.25],\ I^{(2)}_{aCDR} =]0.25; 0.4],\ I^{(3)}_{aCDR} =]0.4; 0.7],\ I^{(4)}_{aCDR} =]0.7; 0.9],\ \text{and}\ I^{(5)}_{aCDR} =]0.9; 1] \quad (6)$$

Each interval of values corresponds to a level of progress of the disease as described in section III, from healthy subject with a CDR value comprises into $I^{(1)}_{aCDR}$ to advanced glaucoma with area-based CDR value comprises into $I^{(5)}_{aCDR}$. However, when area-based CDR value reaches an intermediate interval of values, we assign another clinical feature to inspect along other assigned intervals, according to the clinical aspect of glaucoma. For example, the ISNT rule is computed in $\{aCDR \in I^{(2)}_{aCDR}\}$ instance, corresponding to an eventual early glaucoma. Obedience or not of the rule allows to distinguish the pathological cases belonging to this interval of study, corresponding to an early presence of glaucoma. Likewise, the diameter-based CDR *vCDR* operates in $\{aCDR \in I^{(3,4)}_{aCDR}\}$ instance, corresponding to an eventual more advanced glaucoma (for clarification, $I^{(i,j)} = I^{(i)} \cup I^{(j)}$). Reached values on *vCDR* are also divided into the following intervals of study:

$$I^{(1)}_{vCDR} = [0; 0.45],\ I^{(2)}_{vCDR} =]0.45; 0.6],\ I^{(3)}_{vCDR} =]0.6; 0.8],\ \text{and}\ I^{(4)}_{vCDR} =]0.8; 1] \quad (7)$$

These intervals, also specified according to the ICD [17], allows to disseminate the different stages of disease spreading, and manage all clinical cases according to the induced structural changes in the ONH. In accordance with the reached value on diameter-based CDR, we then assign the stage of the disease, or the feature to further inspect for glaucoma assessment. For example, $\{aCDR \in I^{(4)}_{aCDR}$ and $vCDR \in I^{(3,4)}_{vCDR}\}$ instance corresponds to a moderate glaucoma. Likewise, $\{aCDR \in I^{(3)}_{aCDR}$ and $vCDR \in I^{(2,3)}_{vCDR}\}$ allows to detect an eventual early glaucoma with ISNT rule. Moreover, the NRR area appears as being the most discriminative feature to assess the most challenging clinical cases. In this direction, the computation of the *nNRRa* when $\{aCDR \in I^{(4)}_{aCDR}$ and $vCDR \in I^{(3,4)}_{vCDR}\}$ permits to examine the gradual thinning of the NRR in a more precise manner, then assess the rare but existing glaucomatous cases.

In sum, the proposed clinical protocol, established as a hierarchical arborescence according to the relevance of each feature in glaucoma assessment, permits to manage all clinical cases and give indications about the development stage of the neuropathy. All arborescence is established as the ophthalmologist would carry out its examination, to conduct

TABLE II. OBTAINED PERFORMANCE RATES FOR GLAUCOMA SCREENING AND DIAGNOSIS ON DRISHTI-GS1 DATASET.

Metrics	Accuracy	Sensitivity	Specificity	PPV	NPV	F-score
Sivaswamy et al. [51]	80	84.38	72.22	72.22	84.38	77.83
Dutta et al. [74]	83.17	84.13	81.58	88.33	75.61	86.18
Diaz-Pinto et al. [43]	65.34	60	74.19	84	45.09	58.68
SVMs (RBF kernel)	90	90.77	89.23	89.39	90.63	89.99
Proposed method	**93.07**	**98.57**	**80.64**	**92**	**96.15**	**97.34**

an in-depth clinical evaluation of the structural changes caused by the disease and give precise indications about the current progression of glaucoma. Relevance evaluation metrics of the extracted clinical features and the obtained glaucoma assessment within the proposed clinical protocol are drawn in Table II. These results are compared with a few reference, evaluated with the same benchmark dataset, methods of the state-of-the-art for glaucoma screening. Depending on the proposed method, different clinical features are exploited such as the aCDR, the vCDR or the ISNT sectors for ISNT rule.

The method reaches astonishing performance in glaucoma screening, with a global accuracy of 93.07% testifying the capacity of the proposed method to conduct glaucoma assessment. Particularly, sensitivity of 98.57% is reached, assessing the ability of the algorithm to effectively detect glaucomatous subjects across the clinical cohort.

VI. CONCLUSION

In this paper, we alleviated the challenge of fully-automated glaucoma screening and diagnosis from retinal fundus images. Based on a clinical analysis of the structural changes of the ONH induced by the onset and evolution of glaucoma, and a thorough investigation of the clinical benchmarks in the field of ophthalmology, we identified reliable ophthalmic measurements for quantifying the morphological alterations induced by the neuropathy. Hence, our performed algorithm automatically extracts such measurements, using a robust detection and extraction of the ONH, and the parallel computation of two segmentation approaches. From the clinical measurements, we conducted a prior exhaustive study of their sensitivity in the task of glaucoma assessment, and elaborated a clinical protocol appearing as a hierarchical arborescence, to answer the issue of proper management of all clinical cases for accurate glaucoma assessment and grading. Excellent performance has been reached on final evaluation with the computed metrics. As a perspective, we further propose to investigate the clue of articulating the clinical protocol for glaucoma screening with dynamic intervals to study, and enhance our ability to generalize the process of glaucoma assessment. Such adaptive features, taking into account important parameters correlated with retinal image acquisition or patient meta-data, would enable to overcome the presence of false-positive or false-negative outcomes within the cohort for more accurate glaucoma screening.

REFERENCES

[1] Harry A Quigley and Aimee T Broman. The number of people with glaucoma worldwide in 2010 and 2020. British journal of ophthalmology, 90(3):262–267, 2006.

[2] Sharon Kingman. Glaucoma is second leading cause of blindness globally. *Bulletin of the world Health Organization*, 82:887–888, 2004.

[3] Pierre-Maxime Lévêque, Pierre Zéboulon, Emmanuelle Brasnu, Christophe Baudouin, and Antoine Labbé. Optic disc vascularization in glaucoma: value of spectral-domain optical coherence tomography angiography. *Journal of ophthalmology*, 2016, 2016.

[4] Bao Jian Fan, Dan Yi Wang, Louis R Pasquale, Jonathan L Haines, and Janey L Wiggs. Genetic variants associated with optic nerve vertical cup-to-disc ratio are risk factors for primary open angle glaucoma in a us caucasian population. *Investigative ophthalmology & visual science*, 52(3):1788–1792, 2011.

[5] Muhammad Salman Haleem, Liangxiu Han, Jano Van Hemert, and Baihua Li. Automatic extraction of retinal features from colour retinal images for glaucoma diagnosis: a review. *Computerized medical imaging and graphics*, 37(7-8):581–596, 2013.

[6] Jagadish Nayak, Rajendra Acharya, P Subbanna Bhat, Nakul Shetty, and Teik-Cheng Lim. Automated diagnosis of glaucoma using digital fundus images. *Journal of medical systems*, 33(5):337, 2009.

[7] Jun Cheng, Jiang Liu, Yanwu Xu, Fengshou Yin, Damon Wing Kee Wong, Ngan-Meng Tan, Dacheng Tao, Ching- Yu Cheng, Tin Aung, and Tien Yin Wong. Superpixel classification based optic disc and optic cup segmentation for glaucoma screening. *IEEE transactions on medical imaging*, 32(6):1019–1032, 2013.

[8] Pranjal Das, SR Nirmala, and Jyoti Prakash Medhi. Diagnosis of glaucoma using cdr and nrr area in retina images. *Network Modeling Analysis in Health Informatics and Bioinformatics*, 5(1):3, 2016.

[9] Andres Diaz-Pinto, Sandra Morales, Valery Naranjo, and Amparo Navea. Computer-aided glaucoma diagnosis using stochastic watershed transformation on single fundus images. *Journal of Medical Imaging and Health Informatics*, 9(6):1057–1065, 2019.

[10] Amed Mvoulana, Rostom Kachouri, and Mohamed Akil. Fully automated method for glaucoma screening using robust optic nerve head detection and unsupervised segmentation-based cup-to-disc ratio computation in retinal fundus images. *Computerized Medical Imaging and Graphics*, 77:101643, 2019.

[11] JR Harish Kumar, Chandra Sekhar Seelamantula, Yogish Subraya Kamath, and Rajani Jampala. Rim-to-disc ratio outperforms cup-to-disc ratio for glaucoma prescreening. *Scientific reports*, 9(1):1–9, 2019.

[12] Anum A Salam, Tehmina Khalil, M Usman Akram, Amina Jameel, and Imran Basit. Automated detection of glaucoma using structural and non structural features. *Springerplus*, 5(1):1519, 2016.

[13] Noga Harizman, Cristiano Oliveira, Allen Chiang, Celso Tello, Michael Marmor, Robert Ritch, and Jeffrey M Liebmann. The isnt rule and differentiation of normal from glaucomatous eyes. *Archives of ophthalmology*, 124(11):1579–1583, 2006.

[14] Simon K Law, Helen L Kornmann, Naveed Nilforushan, Sasan Moghimi, and Joseph Caprioli. Evaluation of the "is" rule to differentiate glaucomatous eyes from normal. *Journal of glaucoma*, 25(1):27–32, 2016.

[15] Jayanthi Sivaswamy, S Krishnadas, Arunava Chakravarty, G Joshi, A Syed Tabish, et al. A comprehensive retinal image dataset for the assessment of glaucoma from the optic nerve head analysis. *JSM Biomedical Imaging Data Papers*, 2(1):1004, 2015.

[16] Ivo Soares, Miguel Castelo-Branco, and Antonio MG Pinheiro. Optic disc localization in retinal images based on cumulative sum fields. IEEE journal of biomedical and health informatics, 20(2):574–585, 2015.

[17] Vision: The journal of the missouri optometric association. new and revised icd-9 codes for glaucoma. https://www.moavision.org/new-and-revised-icd-9-codes-for-glaucoma.html